PIV experiment on a water tornado flow for environmental purification

Kazuo Ohmi*

[1]Department of Information Systems Engineering, Osaka Sangyo University, Daito, Osaka, Japan
*corresponding author: ohmi@ise.osaka-sandai.ac.jp

Abstract The 3D velocity field of an artificial water tornado flow generated by a powered water circulatory system (PCS) for ecological application is investigated by tomographic PIV experiment. The water circulatory system aims to promote circulation of deoxygenated bottom layer water in closed water areas such as lakes, ponds and reservoirs. Full 3D-3C flow analysis of the tornado flow in a cross-sectional volume along its vertical axis is presented. Some considerations about the practical design of the circulatory system are made regarding the impeller setup with a view to improved pump-up efficiency.
Keywords: Environmental water purification, Artificial water tornado, Tomographic PIV, 3D flow measurement

1 Introduction

Conservation of clean environment in closed water areas such as lakes, ponds and reservoirs is highly important for healthy growth of human and other organisms and maintenance of our ecosystem. From such a point of view, one of the most basic methods to prevent deterioration of water environment is the forced removal or circulation of deoxygenated bottom water in such closed water areas. There have been some conventional measures to do this task, most of which are technically straightforward (e.g. dredging, aeration and injection of purified water) but consume considerable power energy. By contrast, one of the recent but less known techniques called Powered Circulation System or PCS (Environment Measurement Services Inc. [1]) is based on a simple and energy efficient method that uses an artificial tornado flow generated by a rotating submerged impeller. Some earlier works attempt experimental approaches by using stereoscopic (2D-3C) PIV analysis of the artificial tornado flow in the PCS (Hanari and Sakakibara [2], Ohmi et al. [3]) or tomographic (3D-3C) PIV analysis [4] but to enhance the practicality of this new method, more detailed and systematical experimental data are required.

Among various experimental techniques, tomographic PIV [5] is still a powerful and useful 3C-3D measurement tool that combines a classical optical signal processing technique with a robust 3D image reconstruction procedure. Typically, it uses the scheme of multiplicative algebraic reconstruction technique like MART [6] or SMART [7] to reconstruct a 3D volumetric image of distribution of seed particles in the flow and then, a 3D cross correlation technique to estimate the displacement and thus velocity of fluid flow. This new trend PIV technique has been already applied to the experimental flow analysis of the PCS [4] but the PIV system used in this earlier experiment had a couple of technical drawbacks that will be improved in the present work. In the aspect of hardware, the earlier PIV system used 3 high speed cameras with relatively low resolution and low sensitivity, whereas the new system replaces these old three cameras with four more up-to date high speed cameras with improved resolution and sensitivity. At the same time, in the aspect of software, the new system adopts both the MART and SMART algorithms to reconstruct the 3D images of seed particles and the multi-pass recursive cross correlation algorithm to recover the 3D velocity field.

Another objective of the present work is continued data accumulation for the optimum design of PCS system parameters, especially the submerged impeller size and configuration as well as the impeller speed and underwater depth. To meet these objectives, the present tomographic PIV experiment aims to understand the mechanism of the onset of the water tornado flow and the practical reproducibility of the tornado rise flow with pump-up efficiency of bottom layer water.

2 Experimental Setup

To simulate a natural close water area with rather confined geometry, an octagonal water tank has been employed after the reference study of Hanari and Sakakibara [2]. This water tank is made of transparent acrylic glass plate of 12mm thickness and has an octagonal cross section with 352 mm side length (this leads to 805 mm distance between two opposite parallel sides and 915 mm distance between two opposite corners) and 1000 mm height as shown in Figure 1 (a). The water level in this tank is usually 950 mm. The impeller

model for tornado generation is newly designed for the present experiment. The new impeller model has still a double decker structure consisting of upper and lower bane elements but its dimension is slightly enlarged with respect to the earlier model [3][4] in terms of outer diameter and bane tip width and height as depicted in Figures 1 (c), (d) and (e). The upper and lower impeller elements have both four vanes in circumferential direction. Each vane of the lower element is incident at 45˚, while that of the upper element is at 90˚ with respect to the horizontal plane. In addition, the four vanes of the upper and the lower impeller elements are connected with a staggered phase angle of 45˚. This impeller model is set under water surface at 30 to 60 mm depth position in the center of the water tank and is driven by a DC servo motor (Oriental Motor Co. Ltd.: BLHM450K) above water. The impeller and the servo motor are connected by a vertical axis but separated by a 3 mm thick transparent plate, which covers the entire surface of the water surface and works as a surface wave canceller. Figure 1 (b) is a schematic diagram of the layout of this water tank with a submerged double decker impeller. The upper and lower impeller elements are both 50 mm in outer diameter, 6 mm in axial thickness and have four vanes in circumferential direction. The planar vanes of the lower element are incident at 45˚, while those of the upper element are at 90˚. In addition, the four vanes of the upper and lower impeller elements are placed with a staggered angle of 45˚.

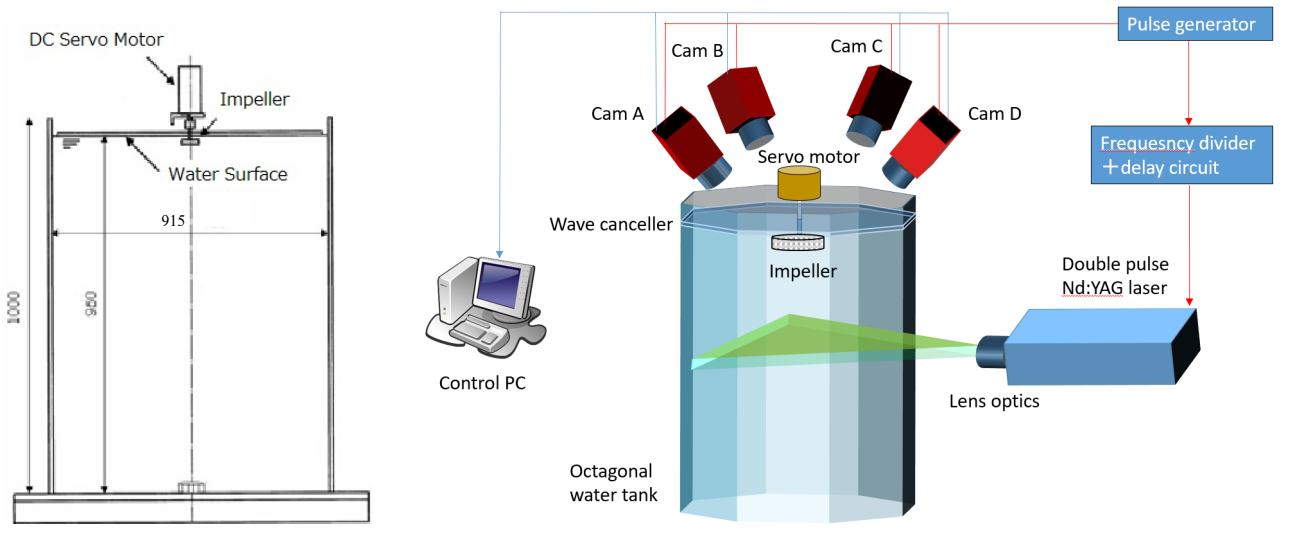

(a) Water tank side view (b) Pulse laser optics and high speed cameras

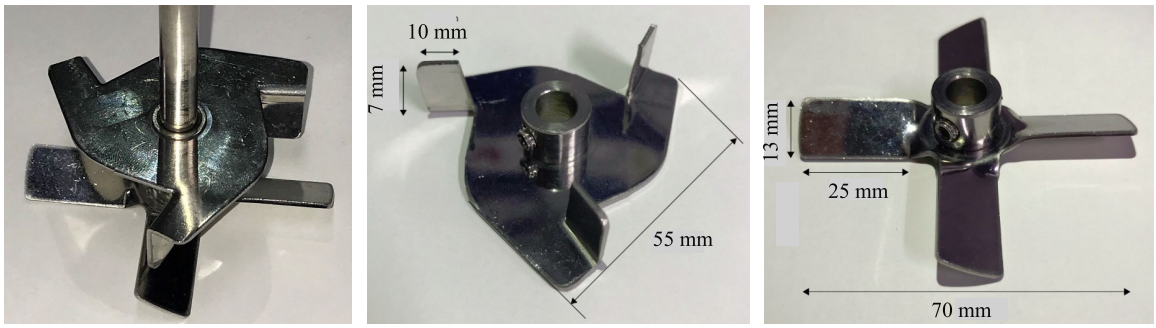

(c) Double-decker impeller (d) Upper impeller element (e) Lower impeller element

Fig. 1 Schematic of experimental setup

The seeding in water for the PIV experiment is done by using fine high-porous particles (Mitsubishi Chemical: Sepabeads SP2MGS) of about 120 μm mean diameter as shown in Figure 2, which are mostly deposited evenly on the bottom surface of water tank at each startup of the PIV experiment. A 15 mm thick laser light sheet generated by a double pulse Nd:YAG laser (New Wave Research: Solo 120) with cylindrical lens optics enters the middle height horizontal cross section of water tank and illuminates the motion of seed

particles in the observation volume. Four high speed cameras (Baumer: HXC20) are installed above the water surface of the tank and oriented downwards to record the seed particle images in the PIV measurement volume. Specifically, the four cameras are fixed with a depression angle of about 60˚ and aimed at the cross-sectional center of water tornado visible in the view field of each camera. In the top view of the PIV experiment, the four high speed cameras are arranged circumferentially along the octagonal side walls of the water tank with an angular interval of about 90˚ from one another. Detailed specifications of the pulse laser sheet and the high speed camera image recording are summarized in Table 1.

A pulse generator (NF Corp.: DF1906) operated at 112 Hz generates the master trigger pulse which is used directly to trigger the shutter of the four high speed cameras externally. On the other hand, this master pulse frequency is divided down to 14 Hz with some additional delays by using a delay pulse generator (Kanomax: 1877) and supplied to trigger the double pulse Nd:YAG laser. Thus, the four high speed cameras at 112 Hz synchronized frame rate are configured to record only one pair of PIV images in every eight sequential image recordings. These time series PIV images are recorded real-time in the main memory of the control PC but thereafter transferred to the external memory devices for the tomographic PIV calculation. The setup arrangement of the water tank, pulse laser optics, high speed cameras and the synchronization devices are schematically illustrated in Figure 1 (b).

In the actual PIV experiment, the water tornado generated by the PCS is first located from outside of the water tank as well as in the view field of the cameras and image recording is only initiated after confirming the proper location of the center of tornado cross section in the camera view field because the central axis of the artificial tornado in the water tank is not constantly stable but slowly swirling around the rotating impeller above. In addition, the tornado flow itself undergoes a slow repetition cycle of strong concentration of vorticity along the tornado axis. Considering all these uncertain experimental factors in the artificial water tornado, tomographic PIV analysis of the tornado flow in the present work is carried out at one limited experimental condition of the submerged impeller, namely the 30 mm impeller depth below water surface and impeller rotation speed 600 rpm. This rotation speed corresponds to Reynolds number of about 32000.

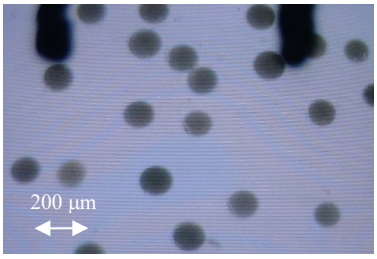

Model	Mitsubishi SP2MGS
Material	High porous polymer
Specific gravity	1.09
Mean diameter	120 [μm]

Fig. 2 Seed particles used in the PIV experimental

Table 1 Specifications of PIV laser and high speed camera

High speed cameras	Baumer: HXC20
Number of cameras	4
Image resolution	2048H×1088V
Pixel size	5.5×5.5 μm
Pixel depth	8 bits
Maximum frame rate	337 Hz at full resolution
Operated frame rate	112 Hz
Laser model	New Wave Research: Solo 120
Laser type	Double pulse Nd:YAG (120 mJ)
Maximum repetition rate	15 Hz
Operated repetition rate	14 Hz
Laser sheet thickness	15 mm

The camera calibration is carried out by using a direct linear transformation (DLT) scheme [8]. A non-coplanar calibration plate with three depth levels at 2 mm spacing is set in the water tank at the exact height of the laser light sheet for PIV image recording. Totally 120 calibration dots with 10 mm vertical and horizontal spacing are printed on the plate and still images of these dots are recorded by the four high speed cameras prior to the PIV experiment. The centroid of calibration dots in each recorded image is calculated using the dynamic threshold binarization [9] and the weighted averaging algorithms.

In the tomographic reconstruction of 3D particles at each frame of the recorded image, the reconstruction volume of 168×168×16 mm^3 in physical space is discretized into 560×560×80 voxels, the single voxel size being 0.3×0.3×0.2 mm^3. The reconstruction algorithms currently in use is the standard MART [6] with minor refinement [10] as well as the improved SMART [7] for reducing the computational loads. After the tomographic reconstruction in voxel space is completed, 3D displacement of particles at each interrogation volume is calculated by means of 3D cross correlation analysis. The actual 3D cross correlation scheme used in the present work is the parallel projection correlation (PCC) [11] which is regarded as multilayer 2D cross correlation performed in three orthogonal directions. The interrogation volume size is 32×32×16 voxels with overlapping ratios of 75×75×50 % in x, y and z direction. More detail about the parameterization of the MART/SMART reconstruction and the PPC cross correlation is summarized in Tables 2 and 3.

Table 2 MART reconstruction parameters

Number of iterations	30
Relaxation parameter	1.0
Reconstruction volume	168×168×16 mm^3
Number of voxels	560×560×80
Single voxel size	0.3×0.3×0.2 mm^3

Table 3 3D cross correlation parameters

3D correlation scheme	PPC
Interrogation mask size	32×32×16 pix
Interrogation interval	8×8×8 pix

3 Experimental Results

3.1 Flow visualization experiment

The earlier flow visualization experiment work by the present author and his co-workers [4] shows that this type of artificial water tornado undergoes, after a certain period of initial development from bottom of water, a highly characteristic and cyclic evolution of vortex flow as shown in Figure 3. This cycle of evolutions consisting of development, breakdown-dissipation and reorganization of vortex flow is repeated autonomously with a relatively long period of about 2 to 5 minutes depending mainly on the impeller conditions. From the startup of the impeller rotation to the establishment of the first vortex flow in full development, it takes another 2 to 5 minutes. In this cyclic evolution, the present tomographic PIV experiment is focused on the 3D flow topology of the full development and breakdown-dissipation phases of the vortex flow.

3.2 Tomographic reconstruction

Figure 4 shows a sample shot of instantaneous particle images of the water tornado in full development recorded by four high speed cameras with 2048×1088 pix resolution. The recorded images of the cameras always capture this type of cross sectional view of water tornado observed from above with an inclined angle of 30˚. One more point to be noted is that the location of tornado center in each camera view field is variant dependent not only on the camera axis orientation but also on the elapse of time because the tornado axis is slowly swirling around the rotating impeller at the top. This swirling motion is so influential in the camera view field that the tornado center comes often outside the view field. Therefore, the PIV image recording has to be started after careful monitoring of the tornado center in each camera's view field.

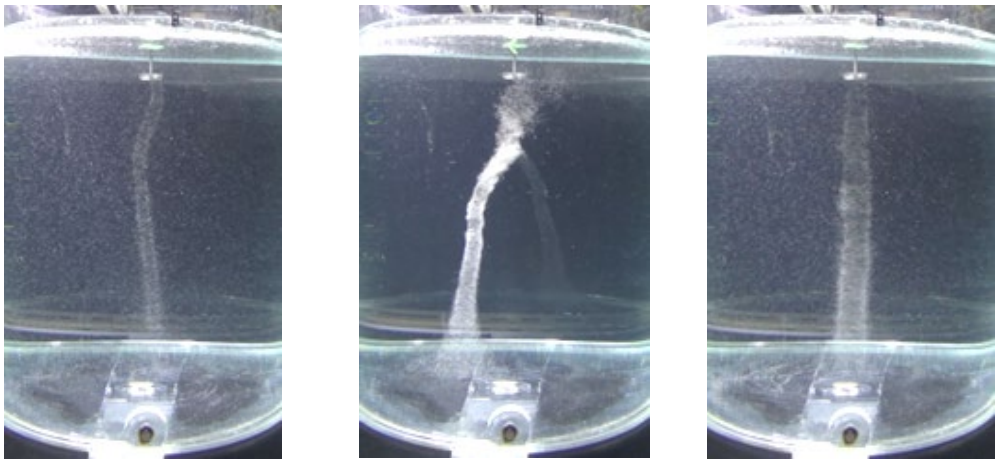

(a) Full development (b) Breakdown-dissipation (c) Reorganization

Fig. 3 Cyclic evolution of water tornado flow

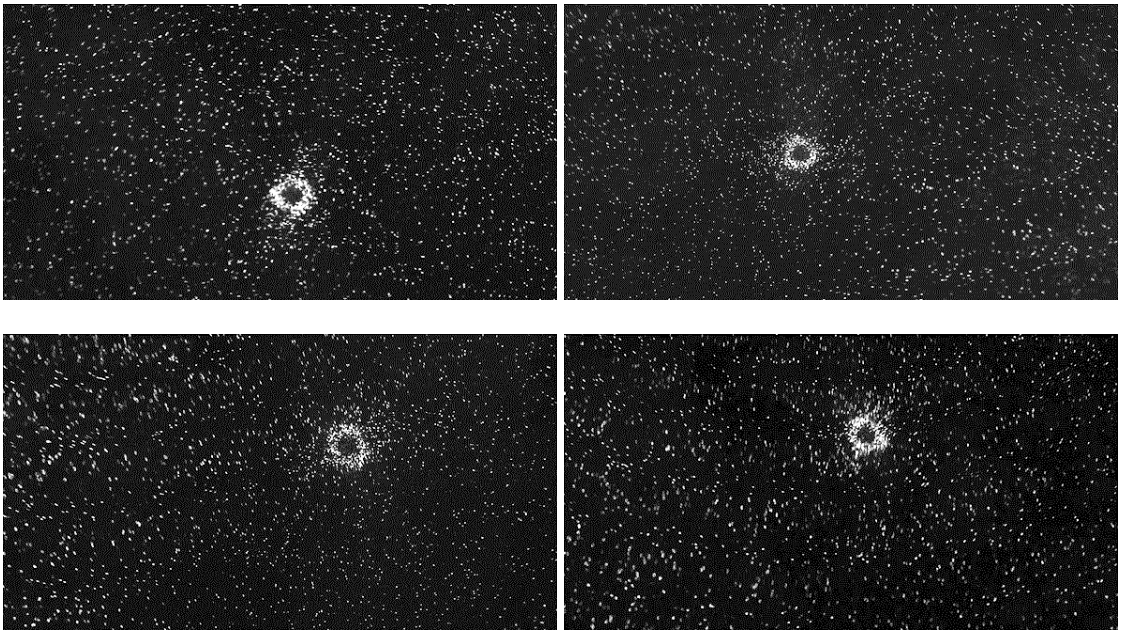

Fig.4 Sample shot of particle images of tornado cross section recorded by four high speed cameras

In the present PIV experiment, the tomographic reconstruction is carried out by using the raw camera recorded images without any post-processing, because they are generally well contrasted and free from background noise. The reconstruction volume is relatively small with respect to the camera recorded image (the main surface of the reconstruction volume is about 1/3 of the size of the recorded image) because the reconstruction at peripheral areas of the tornado requires a certain extent of image resolution. Figure 5 shows two sequential shots of tomographic reconstruction results of the water tornado in the cross sectional volume. Similarly to Figure 4, the tornado flow in these results is in the full development stage. Obviously, the water tornado in full development stage is characterized by a high degree of particle concentration in the peripheral area of the tornado. As a result, the water tornado in 3D perspective gives rise to appearance of a tube of particle concentration. Most probably this high degree of concentration indicates a very strong velocity gradient along the outer periphery of the tornado.

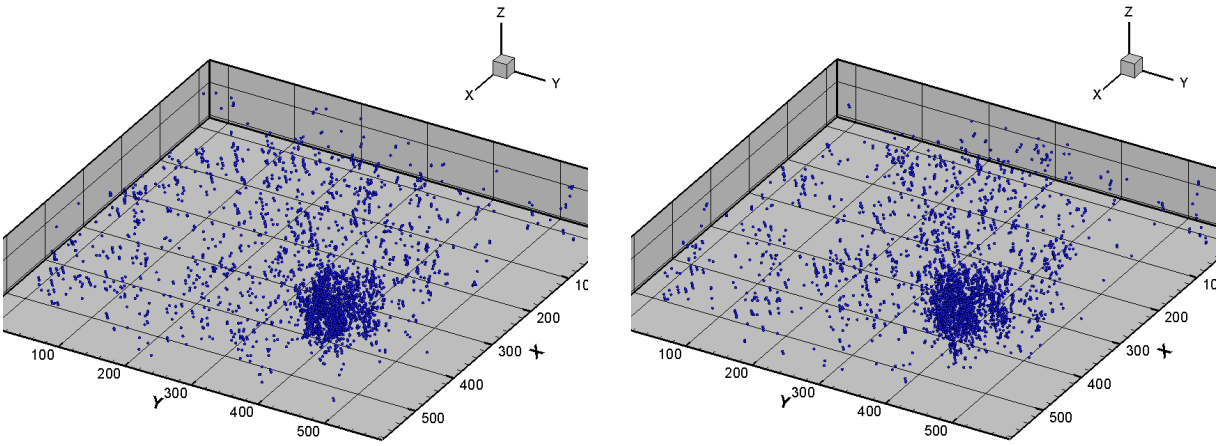

(a) t=0 [s] (b) t=1/14 [s]

Fig. 5 Two sequential shots of tomographic reconstruction results in the measurement volume

3.3 Flow velocity distribution in 3D space

Figure 6 presents a typical set of tomographic PIV results showing the same shots of 3D velocity distribution around the tornado flow at full development stage. The first diagram (a) shows a plain 3D velocity map with the indication of a highly concentrated and spinning tornado flow by a red circle, while the rest of three diagrams (b), (c) and (d) show color contour distribution of out-of-plane velocity at the top, middle and bottom surfaces of the measurement volume. In any case, the measurement volume size is 168×168×16 mm^3 in physical scale, which is discretized into a 560×560×80 voxel grid, of which the single voxel size is 0.3×0.3×0.2 mm^3 in x, y and z directions.

As seen clearly from these 3D velocity maps, the water tornado at full development stage forms a highly concentrated ring shape high speed flow region in the periphery of the tornado main body. And this ring shape region corresponds exactly the densely concentrated portion in the diagrams of particle distribution of the same flow. This observation probably suggests that the confined high speed flow region in the periphery of tornado is maintained due to the dynamic balance of centrifugal force exerted from inside to outside of the tornado core and the pressure gradient force exerted oppositely. And this balance is broken if the centrifugal force exceeds the pressure gradient as the rotational flow speed in the periphery is in excess of a certain limit. This corresponds to the breakdown of the tornado flow. Figure 7 shows two sequential shots of out-of-plane velocity contour in four vertical cross sections surrounding the periphery region of the tornado. Both of these results indicate that the out-of-plane velocity in this periphery region is not consistently upward oriented but alternately variant from upward to downward oriented along the periphery. And same color contour (e.g. red or blue) in these cross sections is seen to spread slantwise in z direction. This means that a rather complex 3D swirling flow with secondary structure is generated in the boundary part of the artificial water tornado at full development stage. By contrast, the water tornado flow at post-breakdown stage (no PIV results is included here) is characterized by a broadly spread and slowly swirling water flux in the central part of the water tank and no distinct figure of a tubular tornado flow is visible any more. In addition, the out-of-plane velocity contour in vertical cross sections does not show alternation of upward and downward velocity along the periphery.

4 Conclusion

Tomographic PIV analysis of the water tornado flow generated by a submerged rotating impeller in powered water circulatory system (PCS) was performed using new improved system hardware and software. This type of tornado flow showed highly contrasted characteristics during the full development and post-breakdown stages in terms of observation by conventional flow visualization as well as in the 3D velocity profiles by tomographic PIV experiment. Formation of highly concentrated and rapidly rotating ring-shape flow areas with strong pressure gradient was clearly observed along the periphery of the water tornado flow during the

full development stage, whereas broadly spread and slowly swirling water flux was existent in the central part of water tank and no distinct figure of a tubular tornado flow was visible during the post-breakdown stage. It was also observed that in the full development stage of tornado flow, the out-of-plane velocity in the periphery region was not consistently upward oriented but alternately variant from upward to downward oriented along the periphery.

Acknowledgements

The present author is grateful to two undergraduate students, A. Sakata and M. Hamana, of Osaka Sangyo University for their technical support in the PIV experiment.

References

[1] Environment Measurement Services Inc. (2009) EcoFlow document. http://www.ems-kankyo.co.jp/ecoflow/en-punhu.pdf

[2] Hanari T, and Sakakibara J (2010) Dual-plane stereo-PIV study on tornado-like vortex in water (in Japanese). *Journal of Visualization Society Japan*, 30(7), pp 47-54.

[3] Ohmi K, Hiratsuka A, and Sasaki M (2013) Visualization experiment on an artificial tornado flow under density stratified water environment. *Proc. 12th Asian Symposium on Visualization*, 229.

[4] Ohmi K, Tuladhar S (2018) Tomographic PIV analysis of water tornado flow for environmental system application. *Proc. of the 5th International Conference on Experimental Fluid Mechanics*, 1.2.B.

[5] Elsinga GE, Scarano F, Wieneke B, and Van Oudheusden BW (2005) Tomographic particle image velocimetry. *Proc. 6th International Symposium on Particle Image Velocimetry*, S10-1.

[6] Herman GT, and Lent A (1976) Iterative reconstruction algorithm. *Computers in Biology and Medicine*, 6(4), pp 273-294.

[7] Mishra D, Muralidhar K, Munshi P (1999) A robust MART algorithm for tomographic applications. *Numerical Heat Transfer, Part B*, 35(4), pp 485-506

[8] Abdel-Aziz YI and Arara HM (1971) Direct linear transformation from comparator coordinates into object space coordinates in close-range photogrammetry. *Proc. of the ASP Symposium on Close-Range Photogrammetry*, pp 1-18.

[9] Ohmi K, Li HY (2000) Particle-tracking velocimetry with new algorithms. Measurement Science and Technology, 11(6), pp 603-616

[10] Joshi B, Ohmi K, and Nose K (2012) Novel algorithms of 3D particle tracking velocimetry using a tomographic reconstruction technique, *Journal of Fluid Science and Technology*, 7, pp 242-258.

[11] Bilsky A, Dulin V, Lozhkin V, Markovich D, and Tokarev M (2011) Two-dimensional correlation algorithms for tomographic PIV, *Proc. 9th International Symposium on Particle Image Velocimetry*, 2-222.

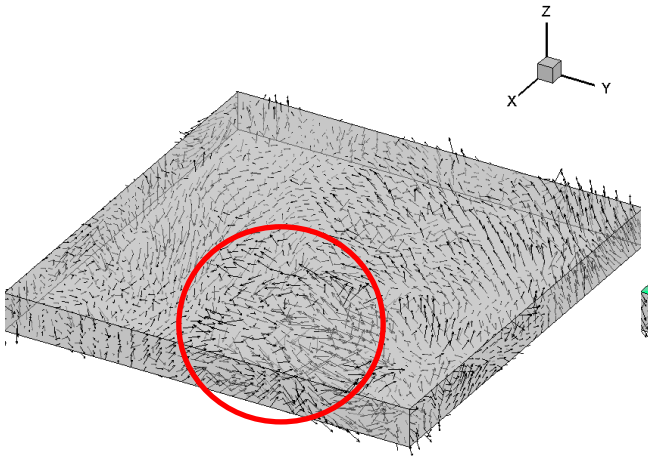

(a) Plain 3D velocity map

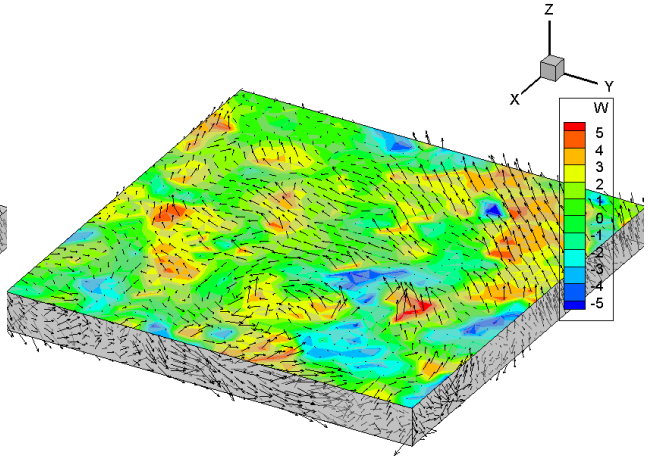

(b) Out-of-plane velocity at top surface of volume

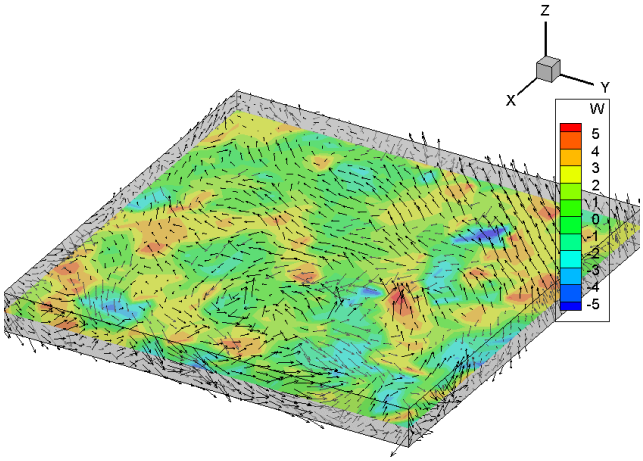

(c) Out-of-plane velocity at mid surface of volume

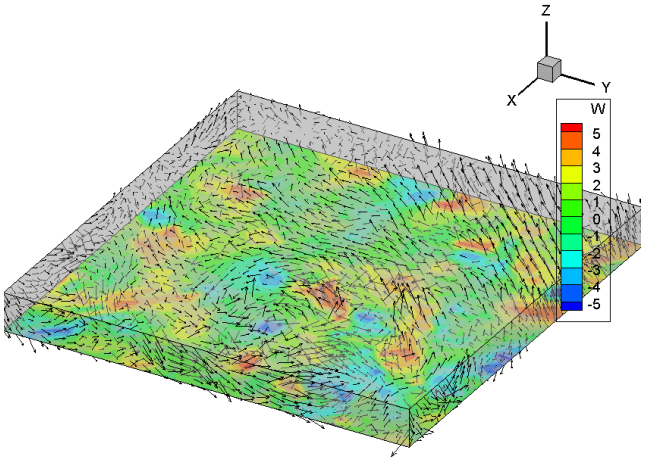

(d) Out-of-plane velocity at bottom surface of volume

Fig. 6 Instantaneous 3D velocity distribution around the water tornado

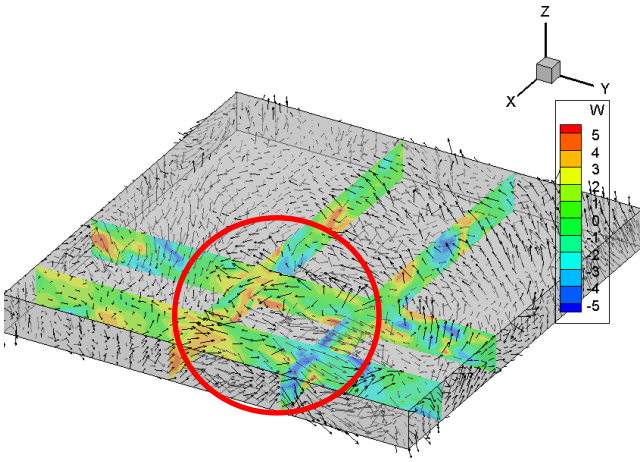

(a) t=0 [s]

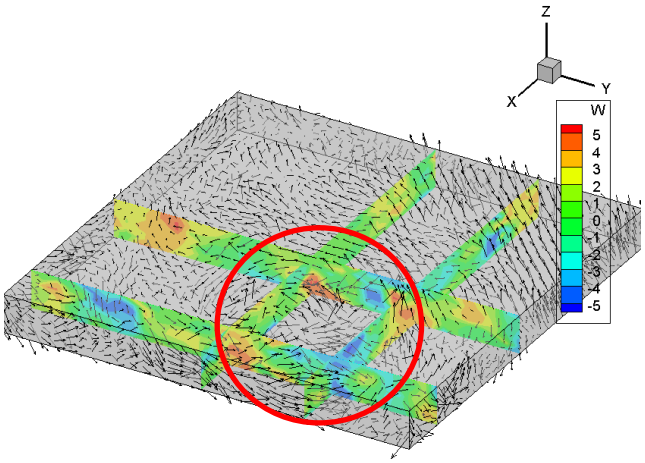

(b) t=1/14 [s]

Fig. 7 Two sequential shots of out-of-plane velocity contour around the water tornado